THE JOURNAL OF PHYSICAL CHEMISTRY C

Article

Cite This: J. Phys. Chem. C 2018, 122, 25339−25348

pubs.acs.org/JPCC

Prevalence of trans-Alkenes in Hydrogenation Processes on Metal Surfaces: A Density Functional Theory Study

Javier Navarro-Ruiz, Damien Cornu, and Núria López*

Institute of Chemical Research of Catalonia, ICIQ, and The Barcelona Institute of Science and Technology, BIST, Av. Països Catalans 16, 43007 Tarragona, Spain

Supporting Information

ABSTRACT: The hydrogenation of triple and double carbon−carbon bonds in C4 molecules containing a single unsaturation has been investigated for the lowest index surfaces of the triad Ni, Pd, and Pt through first-principles simulations. Both low and high hydrogen coverage have been explored to identify the nature of the selectivity found in the experiments. The adsorption behavior of the alkynes and alkenes at high hydrogen concentrations differs from the structures in the infinite dilution-limit coverage which makes a significant contribution to selectivity. Structure sensitivity is also a consequence of the hydrogen coverage, at high contents (111) surfaces cannot trap the C4 molecules efficiently, and thus, the reactivity mainly occurs on the more open (100) surfaces. The combination of fast/slow elementary steps, crucial to eliminate trans-alkenes that are health threatening, is not possible for any of the metals studied, although some metals present slightly better behavior. Our study paves the way towards an integrative analysis of the hydrogenation process that accounts for high surface coverage, preferential adsorption, and kinetic contributions.

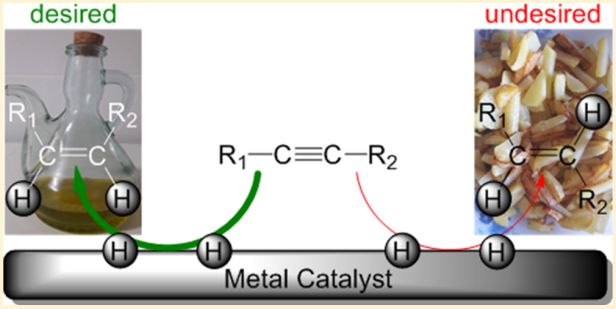

1. INTRODUCTION

Hydrogenation is one of the most traditional catalytic processes and since the 19th century, pioneering works from Wilde[1] have made a landmark in this field. It was not until 1897 when Sabatier and Senderens[2] developed an industrial process by which trace quantities of solid nickel facilitated the hydrogenation of alkenes at low temperatures to transform vegetable oil into margarine.[3,4] Even today, many products such as shortenings, biscuits, pastries, and other baked products contain them. These hydrogenated oils were well recognized for their properties: (i) better rheology than fats (hence easier to spread at lower temperatures);[5] (ii) higher stability than unsaturated and also saturated products (the process of hydrogenation transforms fatty acids that are susceptible to oxidative rancidity); (iii) a more stable production than butter. Thus, since 1920, food industries adopted hydrogenated fats in their production lines and their consumption increased steadily until the 1960s.

The hydrogenation of C−C unsaturated organic compounds[6,7] can take place on several metals: nickel,[8] palladium,[9−16] as well as platinum[17−19] at moderate temperatures and hydrogen pressures. Other transition metals,[20] Ag nanoparticles,[21] and cerium[22] and indium[23] oxides can also carry out the reaction at higher temperatures and in the liquid phase poisoned Pd (Lindlar catalyst[24,25]) is employed. On metals that easily activate H_2,[26−33] the reaction occurs through the Horiuti−Polanyi mechanism[34] where molecular hydrogen is homolytically dissociated on the surface and the hydrogen is transferred sequentially to the organic molecule. However, when starting from an alkyne, if the corresponding alkene is still strongly bound to the surface, a second hydrogenation can occur limiting the selectivity for the semi-hydrogenated product. The loss of selectivity, via over hydrogenation or oligomerization,[35,36] has been analyzed in detail and factors such particle size,[37,38] impurities, or dopants,[39−46] and the addition of molecular selectivity modulators,[47,48] have been shown to regulate selectivity.

The main problem of the hydrogenation process described above is that it preferentially leads to trans-alkenes. As early as 1956, the first evidences that trans fats could be associated with increased risk of coronary heart disease appeared.[49,50] In 1994, the consumption of trans fats, linked to strong evidences in obesity, diabetes, and cancer, was estimated to be the reason behind 30 000 deaths per year in the United States. The ultimate consequence was the establishment of stricter government regulations to minimize the trans-fat consumption, and thus limiting the catalytic processes that can provide less damaging compounds.[51] Therefore, it would be desirable to maximize the obtaining of cis-alkenes, on the one hand, and to minimize the trans-alkenes and/or overhydrogenate them, on the other hand, according to Scheme 1.

Received: July 18, 2018
Revised: October 17, 2018
Published: October 18, 2018

DOI: 10.1021/acs.jpcc.8b06880
J. Phys. Chem. C 2018, 122, 25339−25348

Scheme 1. Reaction Scheme Leading from Alkynes to Alkenes and the Desired Relative Velocities To Maximize the Production of the cis-Compound.

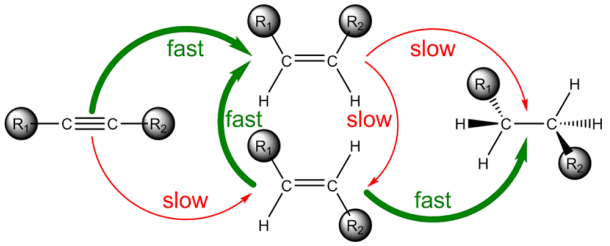

Experiments have shown that when hydrogenating on Pd, trans-alkenes are the most robust semi-hydrogenation products, and thus they remain in the mixture. This can be seen as a preference for the hydrogenation of terminal and cis-alkenes.[52,53] By using temperature-programmed desorption, Doyle et al.[54] have found that C5 and C2 alkanes are not formed as hydrogenation products of the corresponding alkenes on Pd(111) but, in contrast, they do occur on the Pd particles under low-pressure conditions in the presence of subsurface hydrogen. Despite this, first-principles calculations show that the adsorption at high coverage can differ from that of low coverage due to repulsion terms,[55] consistently with experimental infrared reflection absorption spectroscopy data.[56] On Pt(111), cis−trans isomerization of butenes has also been addressed, Li and co-workers[57,58] reported that at low H coverage conversion from the cis to the trans isomer is preferred, whereas on the H saturated surface the reverse appears to be true.

Because the trans fats are typically large molecules with independent functional groups, it is of interest to apply surrogate molecules[59,60] representing the unsaturated moiety as the essential motif. In the present work, by means of density functional theory, we have computed the reaction mechanism for: (i) a collection of surrogates that include C4 organic molecules with C−C triple and double bonds (ii) on three different metals, (iii) with the two most common surface orientations,[61] and (iv) under two different hydrogenation conditions (H-lean and rich) to understand the relative inertness of trans-alkenes under these conditions. Our results constitute the first complete, open (findable, accessible, interoperable, and recyclable, FAIR)[60] database for hydrogenation of alkynes and alkenes.

2. COMPUTATIONAL DETAILS

Density functional theory calculations were performed using the ab initio plane-wave pseudopotential approach as implemented in the Vienna ab initio simulation package (VASP 5.4).[62,63] The Perdew−Burke−Ernzerhof[64] exchange−correlation functional within the generalized gradient approximation was chosen and van der Waals interactions were taken into account through the D2 correction of Grimme[65] in combination with our reparameterized values[66] for the metal surfaces. The innermost electrons were replaced by a projector augmented-wave approach[67,68] while the valence monoelectronic states have been expanded in a plane-wave basis set with a cut-off energy of 400 eV. For bulk calculations, an 11 × 11 × 11 *k*-point mesh was used for all the metals. Within this setup, the optimized face-centered cubic lattice constants were 3.515, 3.945, and 3.975 Å for Ni, Pd, and Pt respectively, in good agreement with the experimental values (Ni: 3.516,[69] Pd:

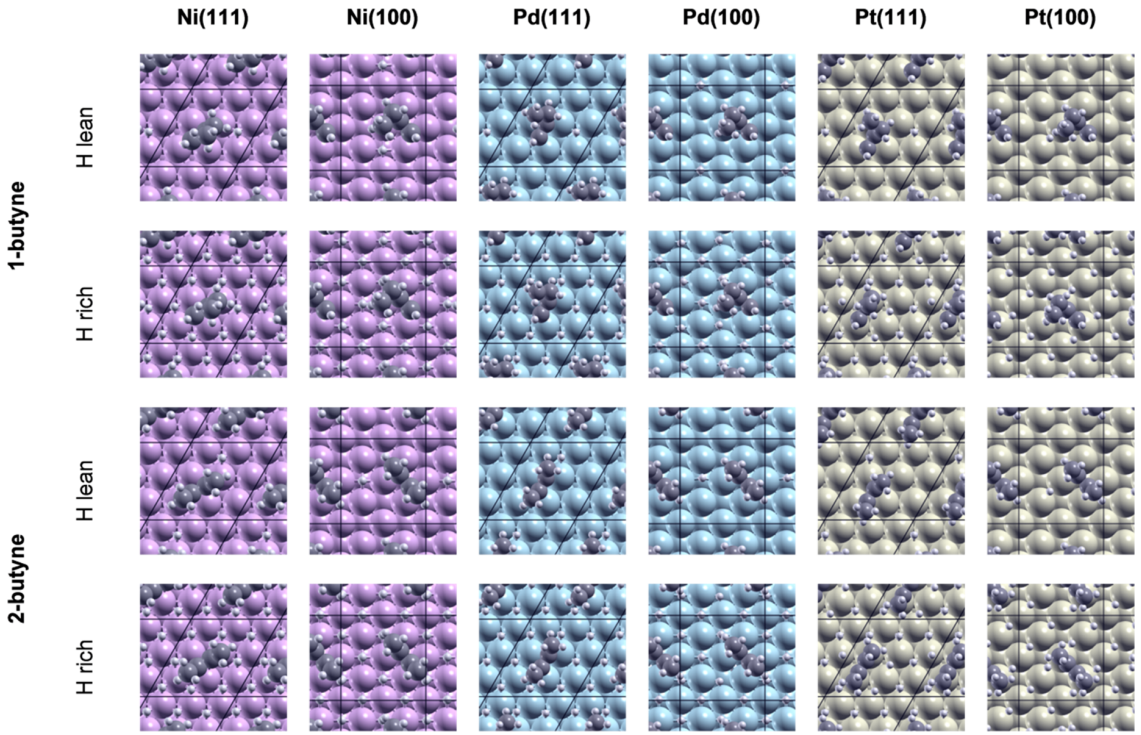

Figure 1. Adsorption structures of all the butynes studied in this work. Color code: Ni (magenta), Pd (cyan), Pt (yellow), C (gray), and H (white). All the structures can be referred in ref 77.

DOI: 10.1021/acs.jpcc.8b06880
J. Phys. Chem. C 2018, 122, 25339−25348

Table 1. Heat Map for Adsorption Energies, E_{ads} in eV, of Butynes as a Function of Hydrogen Coverage.[a]

		Ni(111)	Ni(100)	Pd(111)	Pd(100)	Pt(111)	Pt(100)
1-butyne	H lean	-2.57	-2.86	-2.24	-3.00	-2.70	-3.70
	H rich	-0.54	-1.35	-0.88	-1.69	-0.93	-0.96
2-butyne	H lean	-2.44	-2.84	-2.13	-2.86	-2.61	-3.64
	H rich	-0.46	-1.27	-0.78	-1.56	-0.92	-0.98

weak strong

[a]The scale spans the energies of butynes only.

3.8907,[70] Pt: 3.916 Å[71]). (111) and (100) metal surfaces consist of a five-layer slab (respectively eight and nine atoms per layer and the bottom two ones were frozen) in a $p(3 \times 3)$ supercell (with spin polarization on the nickel surfaces). Γ-Centered $5 \times 5 \times 1$ *k*-point[72] mesh was employed, and a vacuum region by at least 10 Å between the periodically repeated slabs was added. Dipole correction along the *z*-direction has been considered,[73] and transition states were located by the Climbing Image version of the nudged elastic band, CI-NEB, method[74,75] and were proven to show a single imaginary frequency by the diagonalization of the numerical Hessian with a step of 0.01 Å. All structures have been uploaded to the ioChem-BD database[76] and can be consulted in the following link.[77]

3. RESULTS

3.1. Adsorption of Butynes and Butenes on the Low Energy Surfaces. Here, the adsorption of all the C4 compounds (1- and 2-butyne, 1-butene, *cis*- and *trans*-2-butene, and isobutene) on Ni, Pd, and Pt(111) and (100) surfaces at low 0.11−0.13 ML and high 1.00 ML H coverage, depending if there is a single H atom or an entire H monolayer adsorbed per unit cell, respectively, is presented. The adsorption structures and the corresponding energies for butyne (and butene) isomers are summarized in Figure 1 and Table 1 (Figure 2 and Table 2), respectively.

The conformation of butynes is similar irrespective of the metal facet, the C≡C is adsorbed with the triple bond occupying a hollow adsorption site. At low H coverage on the (111) surfaces, butynes bind to Pt more strongly than Ni, and this one, in turn, more than Pd. But for the (100) orientation, the binding to Ni and Pd is comparable and stronger than for Pt. Therefore, binding over (100) is stronger than over (111), the energy difference being about 0.35 eV for butynes on Ni but increasing to 0.75 eV for Pd and around 1.00 eV for Pt. This follows the rule that more open surfaces in terms of coordination allow stronger interactions.[78,79] The situation does not particularly change in terms of adsorption geometries but adsorption energies are much smaller at high H coverage. Butynes are adsorbed as described for low hydrogen content except on Pt,[38,80] in this case, in a bridge position. Instead, the binding energies for butynes are small, around 0.5 for Ni and 0.8−0.9 eV for Pd and Pt(111). Therefore, when going from a low to high H coverage the adsorption energies are reduced on an average to 1/3 of the infinite dilution-limit value. For the open surfaces, the adsorption values triple for Ni, double for Pd but only increase slightly for Pt.

For butenes the adsorption differs from that of butynes, in this case, C=C bonds are formed between the two metal atoms in a bridge position. In this point of view, the adsorption energies of butenes are found to be weaker than that of butynes on all the surfaces considered,[6] the fact that follows the valence dependence found by Abild-Pedersen and co-workers.[81] However, a behavior similar to that of butynes at low H coverage is found and the binding is larger going from Ni < Pd < Pt irrespective of the surface orientation. When going to the open surfaces, the adsorption is stronger by 0.2 eV for Ni, slightly lower for Pd, and around 0.3 eV for Pt. At high H coverage, butenes are adsorbed as described for the low hydrogen content, but they are even more weakly bound as it has been seen for butynes. Physisorption energies are retrieved for Pd and Pt(111), thus indicating that for these surfaces desorption will be preferred to highly H-covered surfaces. For the corresponding (100) orientation, the values range from 0.4 for Ni to 0.6−0.8 eV for Pd and Pt except for isobutene that shows lowers values on Pt.

3.2. Semi-Hydrogenation Reaction of Butynes. The hydrogenation reaction on the active metals takes place through the Horiuti−Polanyi mechanism described previously. 384 elementary steps were calculated corresponding to the hydrogenation of all C4 butynes and butenes on the three metal surfaces with the two surface orientations and at both H coverage. All the elementary steps are listed in Table S1. Particularly, in conditions of high coverage, where there are several H atoms around the C4 species, the H attacking the organic moieties is always the closest and is able to carry out the reaction (an example is given in Figure S1). Since the description is very extensive, we have focused on three prototypical molecules: 2-butyne as an example of alkyne and *cis*- and *trans*-2-butene as an example of alkene.

The energy profiles are summarized in Figure 3. All the computed energies are given with respect to the gas-phase organic moiety plus the already adsorbed H atoms and are presented as potential energies, thus, not considering the entropies. Therefore, the comparison between the adsorbed state and the first hydrogen insertion is meaningful when considering the relative activity of the different metals, or hydrogen coverage. In general, the hydrogenation process from 2-butyne to *cis*- and *trans*-2-butene is thermodynamically favorable and particularly at low hydrogen regime, with values between −1.3 and −1.5 eV, whereas in the case of a high H content the values vary between −0.3 and −1.2 eV. In contrast, the lowest energy barriers correspond to the H-rich metal surfaces, ranging from 0.2 to 0.9 eV, while for the case of low H coverage are from 0.4 to 1.2 eV. At high hydrogen coverage conditions, however, H atoms occupy sites where C4 species are typically present and may reduce the adsorption energy, thus affecting hydrogenation. Trying to account for the degree of energy lost due to the presence of the full coverage, one of the reaction networks is evaluated at intermediate H regimes as shown in Figure S2. As it can be seen, these regimes are interspersed between the lowest and the highest, so thermodynamics and kinetics can be interpolated and follow the trends shown above. Hence, to illustrate the role of the zero point vibrational energy (ZPVE), one of the reaction mechanisms considering the ZPVE is reported (see Figure S3

DOI: 10.1021/acs.jpcc.8b06880
J. Phys. Chem. C 2018, 122, 25339−25348

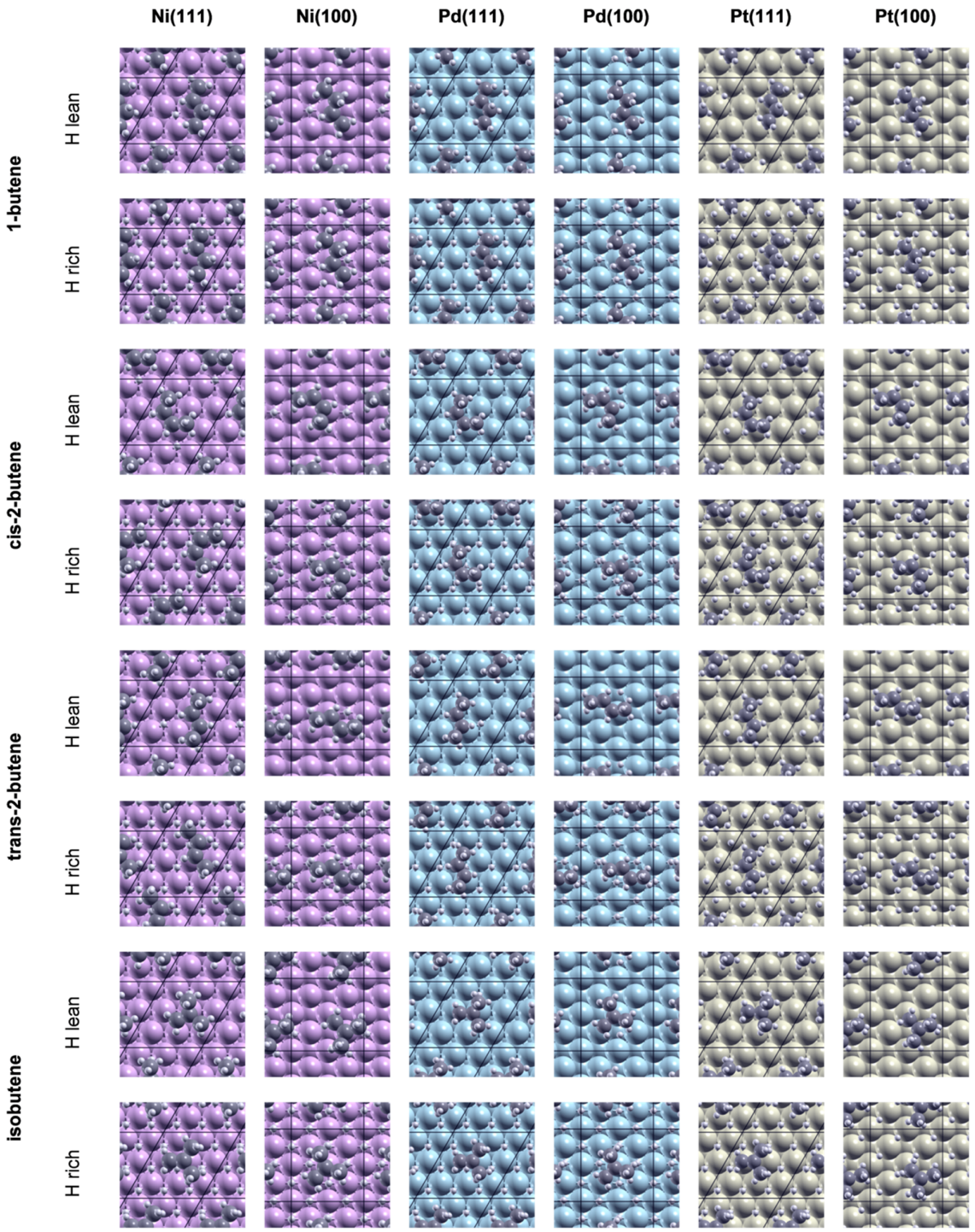

Figure 2. Adsorption structures of all the butenes studied in this work. Color code: Ni (magenta), Pd (cyan), Pt (yellow), C (gray), and H (white). All the structures and can be referred in ref 77.

of the Supporting Information). Because the ZPVE always corresponds to the addition of hydrogen that is activated on the surface, these values are roughly constant, and thus have not been applied to all cases.

Each metal shows preference for obtaining one (or the other alkene) depending on its orientation and hydrogen content. Defining $\Delta E_a^{cis/trans} = E_a^{trans} - E_a^{cis}$, where E_a is the energy barrier of the process (see Figure 3a), for Ni the H-rich (111) and H-lean (100) surfaces give the cis isomer as the major hydrogenation product ($\Delta E_a^{cis/trans} > 0.3$ eV), the H-lean (111) surface gives the trans isomer ($\Delta E_a^{cis/trans} = -0.2$ eV), and finally the H-rich (100) could give both isomers due to the fact that both are very similar in energy. Using Pd, while both orientations at low H coverage preferentially maintains the production of the cis isomer ($\Delta E_a^{cis/trans} > 0.1$ eV), the (111) surface at high H gives the trans isomer as the main

DOI: 10.1021/acs.jpcc.8b06880
J. Phys. Chem. C 2018, 122, 25339−25348

Table 2. Heat Map for the Adsorption Energies, E_{ads} in eV, of Butenes as a Function of Hydrogen Coverage.[a]

		Ni(111)	Ni(100)	Pd(111)	Pd(100)	Pt(111)	Pt(100)
1-butene	H lean	-0.85	-1.11	-1.16	-1.23	-1.39	-1.62
	H rich	-0.29	-0.46	-0.13	-0.77	-0.30	-0.73
cis-2-butene	H lean	-0.86	-1.06	-1.05	-1.24	-1.33	-1.67
	H rich	-0.40	-0.50	-0.31	-0.83	-0.21	-0.74
trans-2-butene	H lean	-0.85	-1.04	-1.07	-1.19	-1.35	-1.65
	H rich	-0.44	-0.43	-0.23	-0.70	-0.45	-0.75
isobutene	H lean	-0.79	-1.08	-1.06	-1.34	-1.40	-1.61
	H rich	-0.34	-0.40	-0.10	-0.65	-0.14	-0.45

weak strong

[a]The scale spans the energies of butenes only.

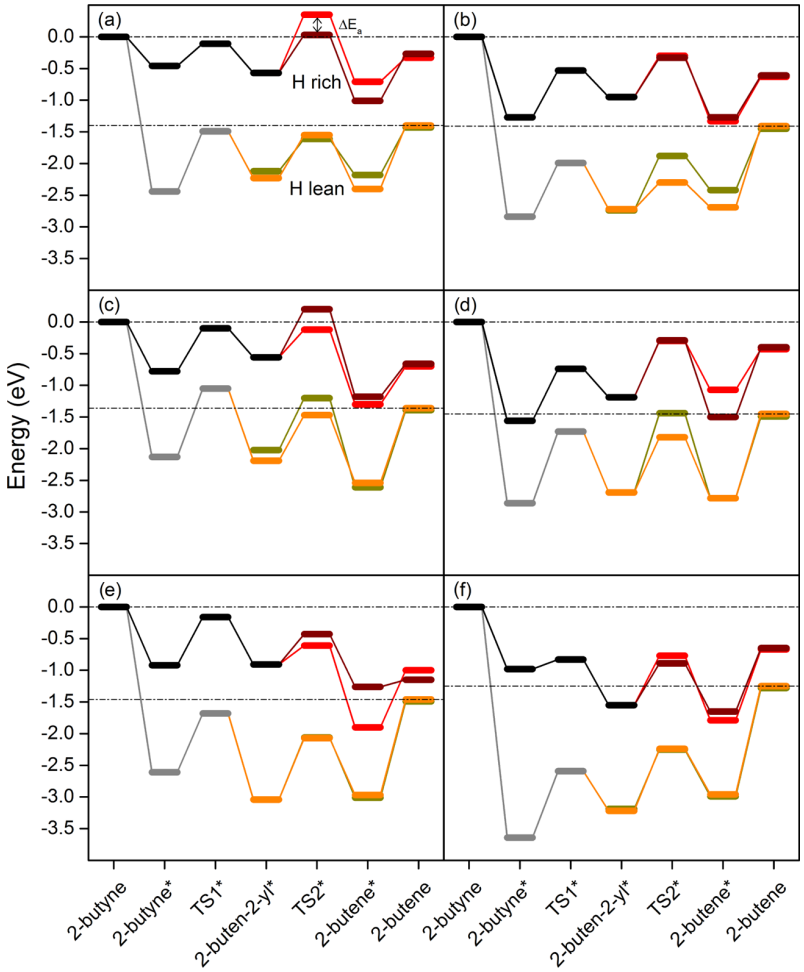

Figure 3. Reaction profiles of 2-butyne semi-hydrogenation to *cis*- and *trans*-2-butene on (a) Ni(111), (b) Ni(100), (c) Pd(111), (d) Pd(100), (e) Pt(111) and (f) Pt(100) surfaces at low (gray for the first common step, orange for cis, and dark yellow for the *trans*-2-butene) and high (black for the first common step, wine for cis, and red for the trans-alkene) hydrogen coverage. Relative energies are referenced with respect to the surface + nH$_{(ads)}$, where n is the number of hydrogen atoms.

hydrogenated product ($\Delta E_a^{cis/trans}$ = −0.3 eV). The remaining situation, H-rich (100), surface could also give both alkenes, although the energy barriers in all cases are high, even more than for Ni. Finally, on Pt, the H-rich (100) facet is the only situation where cis butene is predominant over the trans, whereas the main hydrogenated product in the case of (111) is *trans*-2-butene ($\Delta E_a^{cis/trans}$ = 0.1 and 0.2 eV, respectively).

In the case of partial hydrogenation of 1-butyne to 1-butene and, according to Figure S4, the processes occur both thermodynamically as kinetically analogously to those achieved for obtaining *cis*-2-butene from 2-butyne in all the metals, facets, and coverage studied. In fact, all the energy barriers computed in this work are similar or different depending on what kind of molecule (butynes and butenes), metal (Ni, Pd, and Pt), orientation ((100) and (111)), and coverage (H lean and H rich) is taking part in each reaction. As a result, Ni and Pt are more susceptible to semi-hydrogenation of triple bonds than Pd surfaces because of the low energy barriers and

DOI: 10.1021/acs.jpcc.8b06880
J. Phys. Chem. C 2018, 122, 25339−25348

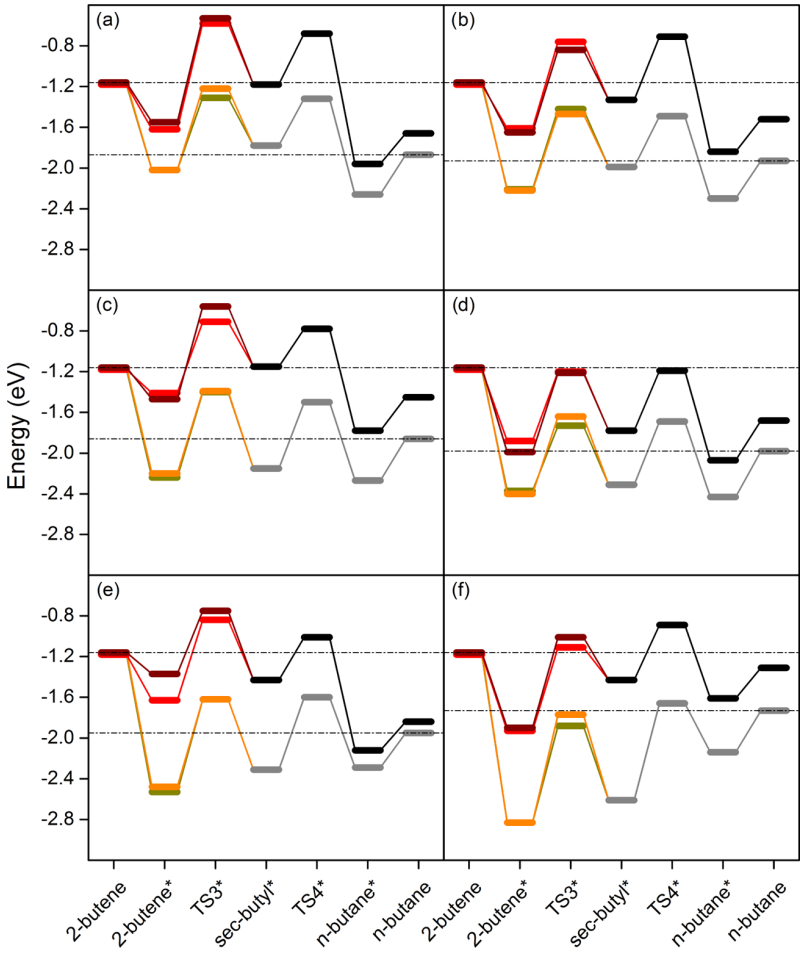

Figure 4. Reaction profiles of *cis*- and *trans*-2-butene hydrogenation to *n*-butane on (a) Ni(111), (b) Ni(100), (c) Pd(111), (d) Pd(100), (e) Pt(111) and (f) Pt(100) surfaces at low (orange for *cis*, dark yellow for the *trans*-2-butene, and gray for the second common step) and high (wine for cis, red for the trans-alkene, and black for the second common step) hydrogen coverage. Relative energies are referenced with respect to the surface + $n\mathrm{H}_{(ads)}$, where *n* is the number of hydrogen atoms.

principally at open (100) surfaces, since the alkynes are more strongly adsorbed making the H-insertions surmountable.

3.3. Hydrogenation Reaction of Butenes. Once 2-butyne is partially hydrogenated to *cis*- or *trans*-2-butene, these could further react to give the fully saturated product, *n*-butane. The energy profiles are summarized in Figure 4. In general, this second hydrogenation process is also thermodynamically favorable for all conditions, with reaction energies ranging from 0.6 for Pt(100) to 0.8 eV for Pd(100) at low hydrogen coverage and from 0.1 for the Pt(100) to 0.7 eV for the Pt(111) in the case of high H contents, values that are about half of those obtained for the first hydrogenation process. The most energy-demanding step is always the first H insertion, especially in the case of (111) surface orientations. In addition, it seems that the process is more difficult at high hydrogen regimes and that the adsorption of alkene is the key factor.

On Ni, the reaction takes place preferentially at low H coverage although the different orientations drive the preference for alkene hydrogenation, trans isomer is faster on the (111) surface, while *cis*-2-butene is faster on the open (100) surface ($\Delta E_a^{cis/trans} \approx |0.1|$ eV). At high coverage, H insertions are slower because both surfaces must overcome a first energy barrier of 1.0 and 0.8 eV for the (111) and (100) surfaces, respectively, which is above the adsorption energy. Using Pd(111) at high hydrogen coverage is the one that is more difficult, since the energy barriers of 0.9 and 0.7 eV for the cis and trans isomers, respectively, are also higher than the adsorption energy in line with H-rich Ni surfaces. At low H contents, the hydrogen insertions occur and in a similar rate for both alkenes. For the (100) surface, both coverages present a preference for the *trans*-2-butene hydrogenation, especially the H-lean one ($\Delta E_a^{cis/trans} \approx -0.1$ eV). In the case of Pt, it happens like Ni and H-lean surfaces are where the formation of *n*-butane occurs favorably whilst on H-rich surfaces must overcome energy barriers of 0.6 and 0.8 eV for the cis and trans-alkenes, respectively, located above the E_{ads}.

In the case of 1-butene (to *n*-butane, see Figure S5) and isobutene hydrogenation (to isobutane, see Figure S6), there are no significant differences both thermodynamically as kinetically to those obtained by the cis and trans isomers in all the metals, facets, and coverage studied, and only occasionally the energy profiles are shifted to more negative values. Thus, irrespective of the H regime, Pt(111) surfaces are the only ones in this orientation for which cis isomer hydrogenation clearly takes preference and Pt(100) surfaces

DOI: 10.1021/acs.jpcc.8b06880
J. Phys. Chem. C 2018, 122, 25339−25348

are, in conjunction with Pd(100), suitable for the trans butenes.

3.4. cis−trans Isomerization. The partial hydrogenation of 2-butyne produces both isomers of 2-butene and, in posteriori second hydrogenation, it produces *n*-butane as a fully hydrogenated product. Hence, from the latter H insertion, it is possible to induce a cis−trans isomerization depending on the kinetics of each reaction. To do this, by comparing from Figure 4 the energy barrier for going from *sec*-butyl (the intermediate formed) to *n*-butane and to cis- or trans-alkene it is possible to point out which are the suitable catalysts.

At high H coverage, (111) surfaces give no isomerization because the second transition state (final H insertion, TS4*) is lower in energy than the first one (first H insertion of the alkene, TS3*). In contrast, (100) surfaces could produce the isomerization due to an inversion in the energy barriers (TS3* < TS4*). According to this, Pt(100) and to a lesser extent Ni(100) are the best to enhance isomerization. In Pt, the reaction goes from trans to cis alkene while on Ni the opposite direction is preferred. On Pd(100), on the other hand, both isomerization and hydrogenation processes are competitive as the two reaction energies are very similar. Additionally, there is no energy difference between cis and trans isomers and hence both could be obtained. Regarding low H contents, both Pt orientations are the only ones that can lead to isomerization. On the Pt(100) surface the same path follows as in H-rich; however, on Pt(111) both energy barriers are exactly the same from the *sec*-butyl intermediate and also very close to H insertion, and subsequently they compete. Therefore, Pt(100) is the best candidate for converting trans-alkenes to cis and hence to maximize the preferred isomer.

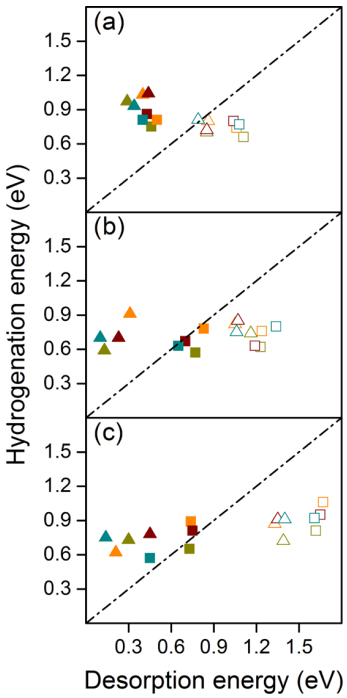

Figure 5. Desorption and hydrogenation energies of 1-butene (dark yellow), *cis*-2-butene (orange), *trans*-2-butene (wine), and isobutene (cyan) on (a) Ni, (b) Pd, and (c) Pt surfaces. Legend: triangles represent (111) surfaces, squares represent (100) surfaces, empty symbols represent low H coverage, and filled symbols represent high H coverage.

4. DISCUSSION

Brønsted−Evans−Polanyi (BEP) relationships[15,48] have been developed between different variables studied and are represented in Figure S7 of the Supporting Information. Although it is true that there is an approximately linear trend between the variables, unfortunately it is not enough precise due to the dispersion of points and this explains why some steps require more energy than others as they follow the thermodynamic request. To understand the resilience of trans-alkenes in these processes, a set of plots are represented in Figure 5. They contain the competing steps: on the *x*-axis the desorption of the alkenes from the surfaces under different conditions is presented while the *y* axis presents the lowest barrier for the hydrogenation of the corresponding alkene. Both terms are affected by zero-point vibrational contributions and entropic ones, but for simplicity they are considered to cancel here. This is equivalent to the approaches of thermodynamic selectivity[30,82] and the competition between over hydrogenation and desorption.[83−85]

The 1:1 rule means that desorption and hydrogenation are equally likely. Therefore, points below the 1:1 line will be further hydrogenated while those above the line indicate that desorption is preferred. The results are crucial to understand the key role of the surface hydrogen content on the selectivity of the process. At low hydrogen contents, hydrogenation is not surface sensitive and none of the metals and orientations inspected could allow a selective hydrogenation process.

However, at high hydrogen content the behavior of the different metals diverges, and the analysis needs to be performed in a more detailed manner. For Ni, the points are clustered in a very small energy and reactivity region presenting very minor differences on (111) and (100) surfaces, so the structure sensitivity found is very small. In stark contrast, Pd and Pt have structure sensitivity and show dispersion on the patterns for desorption and reactivity depending on the surface openness. The structures corresponding to the Pd(100) surface cluster very close to 1:1 rule, but this is slightly less true for Pd(111). As alkenes are very weakly bound to H-rich Pd(111) (around −0.3 eV), the reaction would mainly go through the open (100) surface. On the contrary, the situation for Pt is clearer. The butenes on the close Pt(111) surface are well aligned (not clustered) but located above the 1:1 rule, and therefore, susceptible to desorb, while on the Pt(100) surface three of the alkenes are close in energy and 1:1 rule, and one (isobutene) is separated from these tendencies, resulting to be less reactive.

In summary, the easiest descriptor for semi-hydrogenation, the thermodynamic selectivity, might be employed in the low hydrogen coverage regime but selectivity towards different reactants (cis, trans or terminal) only appears at high hydrogen coverage and only for some surface orientations (structure sensitivity) of some metals. For Ni no significant structure sensitivity exists. Low coverage leads to structure insensitivity for Pd, but at high coverage sensitivity appears (100) surfaces being more active than (111). For these, the terminal alkenes would react first, and the second to be adsorbed would be the cis conformations. This explains while trans are the most resilient and the only ones left once hydrogenation process occurs. On Pt(100) orientation, the ratio of trans would be smaller than on the Pd(100) facet.

DOI: 10.1021/acs.jpcc.8b06880
J. Phys. Chem. C 2018, 122, 25339−25348

5. CONCLUSIONS

We have employed density functional theory on slab models to ascertain the causes of the resilience of trans-alkenes in hydrogenation processes. To this end, two kinds of models at low and high hydrogen coverage have been investigated on the most common hydrogenation metals: Ni, Pd, and Pt in the two most common orientations (111) and (100). We have found that the adsorption energies of alkynes and alkenes are the strong functions of the hydrogen coverage, and indeed organic species adsorption decreases by roughly 2/3 when dense H layers are present. No structure sensitivity is found in the lean H regime for any of the metals explored and the reason is that neither the electronic density nor the adsorption site is compromised. As it can be seen, the stronger the bond the larger the hydrogenation step in agreement with the Brønsted−Evans−Polanyi rules. Indeed, BEP rules appear for the dehydrogenation steps in agreement with previous observations. However, when hydrogen is present, structure sensitivity appears for Pd and Pt and as the organic molecules are weakly adsorbed for the (111) surface the reactions will preferentially occur on the (100) areas of the catalyst. Moreover, on Pd(100) at high coverage terminal and cis-alkenes would react prior to trans conformations, and only on Pt, where the cis−trans proportion would be slightly better. Our work represents the first full set of thermodynamic and kinetic parameters for C4 alkynes and alkene hydrogenations. Such systematic studies pave the way to the understanding of complexity in catalysis as they incorporate surface sensitivity and coverage terms and can indicate potential developments to increase the selectivity towards desired products avoiding those that are potentially harmful.

■ ASSOCIATED CONTENT

Supporting Information

The Supporting Information is available free of charge on the ACS Publications website at DOI: 10.1021/acs.jpcc.8b06880.

Examples of H atoms involved in an H-rich hydrogenation and of a reaction profile as a function of the H coverage and by including ZPVE corrections (Figures S1, S2 and S3, respectively); complete reaction profiles of 1-butyne semi-hydrogenation (Figure S4), 1-butene and isobutene hydrogenations (Figures S5 and S6, respectively), and BEP relations (Figure S7); finally, the list of reaction energies, energy barriers, and imaginary frequencies (Table S1) (PDF).

■ AUTHOR INFORMATION

Corresponding Author

*E-mail: nlopez@iciq.es. Tel: +34 977920237.

ORCID

Javier Navarro-Ruiz: 0000-0002-3604-9338

Núria López: 0000-0001-9150-5941

Notes

The authors declare no competing financial interest.

■ ACKNOWLEDGMENTS

This project has received funding from the European Union's Horizon 2020 research and innovation program under grant agreement No. 686163. The authors acknowledge the MINECO (Grant No. CTQ2015-68770-R) for financial support. The authors also thankfully acknowledge the computer resources at Caesaraugusta and LaPalma, and the technical support provided by BIFI and IAC respectively (RES-ActivityID QCM-2017-3-0015 and QCM-2018-1-0017). D.C. thanks the COFUND Marie Curie program (Grant No. 2014-51588) and MINECO for support through Severo Ochoa Excellence Accreditation (SEV-2013-0319).

■ REFERENCES

(1) v. Wilde, M. P. Vermischte Mittheilungen. *Ber. Dtsch. Chem. Ges.* **1874**, *7*, 352−357.

(2) Sabatier, P.; Senderens, J. B. Action of Hydrogen on Acetylene in Presence of Nickel. *C. R. Hebd. Séances Acad. Sci.* **1899**, *128*, 1173.

(3) Sabatier, P. The Nobel Prize in Chemistry 1912. http://www.nobelprize.org/nobel_prizes/chemistry/laureates/1912/ (accessed April 16, 2018).

(4) Rylander, P. N. Hydrogenation and Dehydrogenation. In *Ullmann's Encyclopedia of Industrial Chemistry*; Wiley-VCH Verlag: Weinheim, Germany, 2000.

(5) Freeman, I. P. Margarines and Shortenings. In *Ullmann's Encyclopedia of Industrial Chemistry*; Wiley-VCH Verlag: Weinheim, Germany, 2000.

(6) Nørskov, J. K.; Bligaard, T.; Rossmeisl, J.; Christensen, C. H. Towards the Computational Design of Solid Catalysts. *Nat. Chem.* **2009**, *1*, 37−46.

(7) Vilé, G.; Albani, D.; Almora-Barrios, N.; López, N.; Pérez-Ramírez, J. Advances in the Design of Nanostructured Catalysts for Selective Hydrogenation. *ChemCatChem* **2016**, *8*, 21−33.

(8) Johnson, A. D.; Daley, S. P.; Utz, A. L.; Ceyer, S. T. The Chemistry of Bulk Hydrogen: Reaction of Hydrogen Embedded in Nickel with Adsorbed CH_3. *Science* **1992**, *257*, 223−225.

(9) Borodziński, A.; Bond, G. C. Selective Hydrogenation of Ethyne in Ethene-Rich Streams on Palladium Catalysts. Part 1. Effect of Changes to the Catalyst During Reaction. *Catal. Rev.* **2006**, *48*, 91−144.

(10) Doyle, A. M.; Shaikhutdinov, S. K.; Jackson, S. D.; Freund, H.-J. Hydrogenation on Metal Surfaces: Why Are Nanoparticles More Active than Single Crystals? *Angew. Chem., Int. Ed.* **2003**, *42*, 5240−5243.

(11) Schauermann, S.; Nilius, N.; Shaikhutdinov, S. K.; Freund, H.-J. Nanoparticles for Heterogeneous Catalysis: New Mechanistic Insights. *Acc. Chem. Res.* **2013**, *46*, 1673−1681.

(12) McCue, A. J.; Anderson, J. A. Recent Advances in Selective Acetylene Hydrogenation Using Palladium Containing Catalysts. *Front. Chem. Sci. Eng.* **2015**, *9*, 142−153.

(13) Vilé, G.; Albani, D.; Nachtegaal, M.; Chen, Z.; Dontsova, D.; Antonietti, M.; López, N.; Pérez-Ramírez, J. A Stable Single-Site Palladium Catalyst for Hydrogenations. *Angew. Chem., Int. Ed.* **2015**, *54*, 11265−11269.

(14) Albani, D.; Shahrokhi, M.; Chen, Z.; Mitchell, S.; Hauert, R.; López, N.; Pérez-Ramírez, J. Selective Ensembles in Supported Palladium Sulfide Nanoparticles for Alkyne Semi-Hydrogenation. *Nat. Commun.* **2018**, *9*, No. 2634.

(15) Andersin, J.; López, N.; Honkala, K. DFT Study on the Complex Reaction Networks in the Conversion of Ethylene to Ethylidyne on Flat and Stepped Pd. *J. Phys. Chem. C* **2009**, *113*, 8278−8286.

(16) Andersin, J.; Honkala, K. DFT Study on Complete Ethylene Decomposition on Flat and Stepped Pd. *Surf. Sci.* **2010**, *604*, 762−769.

(17) Cremer, P. S.; Su, X.; Shen, Y. R.; Somorjai, G. A. Ethylene Hydrogenation on Pt(111) Monitored in Situ at High Pressures Using Sum Frequency Generation. *J. Am. Chem. Soc.* **1996**, *118*, 2942−2949.

(18) Nykänen, L.; Honkala, K. Density Functional Theory Study on Propane and Propene Adsorption on Pt(111) and PtSn Alloy Surfaces. *J. Phys. Chem. C* **2011**, *115*, 9578−9586.

(19) Nykänen, L.; Honkala, K. Selectivity in Propene Dehydrogenation on Pt and Pt_3Sn Surfaces from First Principles. *ACS Catal.* **2013**, *3*, 3026−3030.
(20) Zaera, F. Key Unanswered Questions About the Mechanism of Olefin Hydrogenation Catalysis by Transition-Metal Surfaces: A Surface-Science Perspective. *Phys. Chem. Chem. Phys.* **2013**, *15*, 11988−12003.
(21) Vilé, G.; Baudouin, D.; Remediakis, I. N.; Copéret, C.; López, N.; Pérez-Ramírez, J. Silver Nanoparticles for Olefin Production: New Insights into the Mechanistic Description of Propyne Hydrogenation. *ChemCatChem* **2013**, *5*, 3750−3759.
(22) García-Melchor, M.; Bellarosa, L.; López, N. Unique Reaction Path in Heterogeneous Catalysis: The Concerted Semi-Hydrogenation of Propyne to Propene on CeO_2. *ACS Catal.* **2014**, *4*, 4015−4020.
(23) Albani, D.; Capdevila-Cortada, M.; Vilé, G.; Mitchell, S.; Martin, O.; López, N.; Pérez-Ramírez, J. Semihydrogenation of Acetylene on Indium Oxide: Proposed Single-Ensemble Catalysis. *Angew. Chem., Int. Ed.* **2017**, *56*, 10755−10760.
(24) Lindlar, H. Ein Neuer Katalysator Für Selektive Hydrierungen. *Helv. Chim. Acta* **1952**, *35*, 446−450.
(25) García-Mota, M.; Gómez-Díaz, J.; Novell-Leruth, G.; Vargas-Fuentes, C.; Bellarosa, L.; Bridier, B.; Pérez-Ramírez, J.; López, N. A Density Functional Theory Study of the 'Mythic' Lindlar Hydrogenation Catalyst. *Theor. Chem. Acc.* **2011**, *128*, 663−673.
(26) Neurock, M.; Pallassana, V.; van Santen, R. A. The Importance of Transient States at Higher Coverages in Catalytic Reactions. *J. Am. Chem. Soc.* **2000**, *122*, 1150−1153.
(27) Mitsui, T.; Rose, M. K.; Fomin, E.; Ogletree, D. F.; Salmeron, M. Dissociative Hydrogen Adsorption on Palladium Requires Aggregates of Three or More Vacancies. *Nature* **2003**, *422*, 705−707.
(28) Sheth, P. A.; Neurock, M.; Smith, C. M. A First-Principles Analysis of Acetylene Hydrogenation Over Pd(111). *J. Phys. Chem. B* **2003**, *107*, 2009−2017.
(29) López, N.; Łodziana, Z.; Illas, F.; Salmeron, M. When Langmuir Is Too Simple: H_2 Dissociation on Pd(111) at High Coverage. *Phys. Rev. Lett.* **2004**, *93*, No. 146103.
(30) Segura, Y.; López, N.; Pérez-Ramírez, J. Origin of the Superior Hydrogenation Selectivity of Gold Nanoparticles in Alkyne + Alkene Mixtures: Triple- versus Double-Bond Activation. *J. Catal.* **2007**, *247*, 383−386.
(31) Mei, D.; Neurock, M.; Smith, C. M. Hydrogenation of Acetylene−Ethylene Mixtures over Pd and Pd−Ag Alloys: First-Principles-Based Kinetic Monte Carlo Simulations. *J. Catal.* **2009**, *268*, 181−195.
(32) Bridier, B.; López, N.; Pérez-Ramírez, J. Molecular Understanding of Alkyne Hydrogenation for the Design of Selective Catalysts. *Dalton Trans.* **2010**, *39*, 8412−8419.
(33) Bridier, B.; López, N.; Pérez-Ramírez, J. Partial Hydrogenation of Propyne Over Copper-Based Catalysts and Comparison with Nickel-Based Analogues. *J. Catal.* **2010**, *269*, 80−92.
(34) Horiuti, I.; Polanyi, M. Exchange Reactions of Hydrogen on Metallic Catalysts. *Trans. Faraday Soc.* **1934**, *30*, 1164−1172.
(35) Fiorio, J. L.; López, N.; Rossi, L. M. Gold−Ligand-Catalyzed Selective Hydrogenation of Alkynes into Cis-Alkenes via H2 Heterolytic Activation by Frustrated Lewis Pairs. *ACS Catal.* **2017**, *7*, 2973−2980.
(36) Fiorio, J. L.; Gonçalves, R. V.; Teixeira-Neto, E.; Ortuño, M. A.; López, N.; Rossi, L. M. Accessing Frustrated Lewis Pair Chemistry through Robust Gold@N-Doped Carbon for Selective Hydrogenation of Alkynes. *ACS Catal.* **2018**, *8*, 3516−3524.
(37) Borodziński, A.; Bond, G. C. Selective Hydrogenation of Ethyne in Ethene-Rich Streams on Palladium Catalysts, Part 2: Steady-State Kinetics and Effects of Palladium Particle Size, Carbon Monoxide, and Promoters. *Catal. Rev.* **2008**, *50*, 379−469.
(38) Lee, I.; Delbecq, F.; Morales, R.; Albiter, M. A.; Zaera, F. Tuning Selectivity in Catalysis by Controlling Particle Shape. *Nat. Mater.* **2009**, *8*, 132−138.
(39) Teschner, D.; Borsodi, J.; Wootsch, A.; Révay, Z.; Hävecker, M.; Knop-Gericke, A.; Jackson, S. D.; Schlögl, R. The Roles of Subsurface Carbon and Hydrogen in Palladium-Catalyzed Alkyne Hydrogenation. *Science* **2008**, *320*, 86−89.
(40) Teschner, D.; Révay, Z.; Borsodi, J.; Hävecker, M.; Knop-Gericke, A.; Schlögl, R.; Milroy, D.; Jackson, S. D.; Torres, D.; Sautet, P. Understanding Palladium Hydrogenation Catalysts: When the Nature of the Reactive Molecule Controls the Nature of the Catalyst Active Phase. *Angew. Chem., Int. Ed.* **2008**, *47*, 9274−9278.
(41) Vignola, E.; Steinmann, S. N.; Al Farra, A.; Vandegehuchte, B. D.; Curulla, D.; Sautet, P. Evaluating the Risk of C−C Bond Formation during Selective Hydrogenation of Acetylene on Palladium. *ACS Catal.* **2018**, *8*, 1662−1671.
(42) López, N.; Vargas-Fuentes, C. Promoters in the Hydrogenation of Alkynes in Mixtures: Insights from Density Functional Theory. *Chem. Commun.* **2012**, *48*, 1379−1391.
(43) Galvita, V. V.; Siddiqi, G.; Sun, P.; Bell, A. T. Ethane Dehydrogenation on Pt/Mg(Al)O and PtSn/Mg(Al)O Catalysts. *J. Catal.* **2010**, *271*, 209−219.
(44) Hook, A.; Massa, J. D.; Celik, F. E. Effect of Tin Coverage on Selectivity for Ethane Dehydrogenation over Platinum−Tin Alloys. *J. Phys. Chem. C* **2016**, *120*, 27307−27318.
(45) Saerens, S.; Sabbe, M. K.; Galvita, V. V.; Redekop, E. A.; Reyniers, M.-F.; Marin, G. B. The Positive Role of Hydrogen on the Dehydrogenation of Propane on Pt(111). *ACS Catal.* **2017**, *7*, 7495−7508.
(46) Kogan, S. B.; Schramm, H.; Herskowitz, M. Dehydrogenation of Propane on Modified Pt/θ-Alumina Performance in Hydrogen and Steam Environment. *Appl. Catal., A* **2001**, *208*, 185−191.
(47) Vilé, G.; Almora-Barrios, N.; Mitchell, S.; López, N.; Pérez-Ramírez, J. From the Lindlar Catalyst to Supported Ligand-Modified Palladium Nanoparticles: Selectivity Patterns and Accessibility Constraints in the Continuous-Flow Three-Phase Hydrogenation of Acetylenic Compounds. *Chem. - Eur. J.* **2014**, *20*, 5926−5937.
(48) García-Mota, M.; Bridier, B.; Pérez-Ramírez, J.; López, N. Interplay Between Carbon Monoxide, Hydrides, and Carbides in Selective Alkyne Hydrogenation on Palladium. *J. Catal.* **2010**, *273*, 92−102.
(49) Willett, W. C.; Ascherio, A. Trans Fatty Acids: Are the Effects Only Marginal? *Am. J. Public Health* **1994**, *84*, 722−724.
(50) Ascherio, A.; Katan, M. B.; Zock, P. L.; Stampfer, M. J.; Willett, W. C. Trans Fatty Acids and Coronary Heart Disease. *N. Engl. J. Med.* **1999**, *340*, 1994−1998.
(51) Tarrago-Trani, M. T.; Phillips, K. M.; Lemar, L. E.; Holden, J. M. New and Existing Oils and Fats Used in Products with Reduced Trans-Fatty Acid Content. *J. Am. Diet. Assoc.* **2006**, *106*, 867−880.
(52) Canning, A. S.; Jackson, S. D.; Monaghan, A.; Wright, T. C-5 Alkene Hydrogenation: Effect of Competitive Reactions on Activity and Selectivity. *Catal. Today* **2006**, *116*, 22−29.
(53) Brandt, B.; Ludwig, W.; Fischer, J.-H.; Libuda, J.; Zaera, F.; Schauermann, S. Conversion of Cis- and Trans-2-Butene with Deuterium on a Pd/Fe3O4 Model Catalyst. *J. Catal.* **2009**, *265*, 191−198.
(54) Doyle, A. M.; Shaikhutdinov, S. K.; Freund, H.-J. Alkene Chemistry on the Palladium Surface: Nanoparticles vs Single Crystals. *J. Catal.* **2004**, *223*, 444−453.
(55) Chizallet, C.; Bonnard, G.; Krebs, E.; Bisson, L.; Thomazeau, C.; Raybaud, P. Thermodynamic Stability of Buta-1,3-Diene and But-1-Ene on Pd(111) and (100) Surfaces Under H_2 Pressure: A DFT Study. *J. Phys. Chem. C* **2011**, *115*, 12135−12149.
(56) Stacchiola, D.; Burkholder, L.; Tysoe, W. T. Ethylene Adsorption on Pd(111) Studied Using Infrared Reflection−Absorption Spectroscopy. *Surf. Sci.* **2002**, *511*, 215−228.
(57) Li, J.; Fleurat-Lessard, P.; Zaera, F.; Delbecq, F. Mechanistic Investigation of the Cis/Trans Isomerization of 2-Butene on Pt(111): DFT Study of the Influence of the Hydrogen Coverage. *J. Catal.* **2014**, *311*, 190−198.
(58) Li, J.; Fleurat-Lessard, P.; Zaera, F.; Delbecq, F. Switch in Relative Stability Between Cis and Trans 2-Butene on Pt(111) as a

DOI: 10.1021/acs.jpcc.8b06880
J. Phys. Chem. C 2018, 122, 25339−25348

Function of Experimental Conditions: A Density Functional Theory Study. *ACS Catal.* **2018**, *8*, 3067−3075.
(59) García-Muelas, R.; López, N. Collective Descriptors for the Adsorption of Sugar Alcohols on Pt and Pd(111). *J. Phys. Chem. C* **2014**, *118*, 17531−17537.
(60) Li, Q.; García-Muelas, R.; López, N. Microkinetics of Alcohol Reforming for H_2 Production from a FAIR Density Functional Theory Database. *Nat. Commun.* **2018**, *9*, No. 526.
(61) Barmparis, G. D.; Lodziana, Z.; López, N.; Remediakis, I. N. Nanoparticle Shapes by Using Wulff Constructions and First-Principles Calculations. *Beilstein J. Nanotechnol.* **2015**, *6*, 361−368.
(62) Kresse, G.; Furthmüller, J. Efficiency of Ab-Initio Total Energy Calculations for Metals and Semiconductors Using a Plane-Wave Basis Set. *Comput. Mater. Sci.* **1996**, *6*, 15−50.
(63) Kresse, G.; Furthmüller, J. Efficient Iterative Schemes for Ab Initio Total-Energy Calculations Using a Plane-Wave Basis Set. *Phys. Rev. B* **1996**, *54*, 11169−11186.
(64) Perdew, J. P.; Burke, K.; Ernzerhof, M. Generalized Gradient Approximation Made Simple. *Phys. Rev. Lett.* **1996**, *77*, 3865−3868.
(65) Grimme, S. Semiempirical GGA-Type Density Functional Constructed with a Long-Range Dispersion Correction. *J. Comput. Chem.* **2006**, *27*, 1787−1799.
(66) Almora-Barrios, N.; Carchini, G.; Błoński, P.; López, N. Costless Derivation of Dispersion Coefficients for Metal Surfaces. *J. Chem. Theory Comput.* **2014**, *10*, 5002−5009.
(67) Blöchl, P. E. Projector Augmented-Wave Method. *Phys. Rev. B* **1994**, *50*, 17953−17979.
(68) Kresse, G.; Joubert, D. From Ultrasoft Pseudopotentials to the Projector Augmented-Wave Method. *Phys. Rev. B* **1999**, *59*, 1758−1775.
(69) Bandyopadhyay, J.; Gupta, K. P. Low Temperature Lattice Parameter of Nickel and Some Nickel-Cobalt Alloys and Grüneisen Parameter of Nickel. *Cryogenics* **1977**, *17*, 345−347.
(70) Rao, C. N.; Rao, K. K. Effect of Temperature on the Lattice Parameters of Some Silver−Palladium Alloys. *Can. J. Phys.* **1964**, *42*, 1336−1342.
(71) Arblaster, J. W. Crystallographic Properties of Platinum. *Platinum Met. Rev.* **1997**, *41*, 12−21.
(72) Monkhorst, H. J.; Pack, J. D. Special Points for Brillouin-Zone Integrations. *Phys. Rev. B* **1976**, *13*, 5188−5192.
(73) Makov, G.; Payne, M. C. Periodic Boundary Conditions in Ab Initio Calculations. *Phys. Rev. B* **1995**, *51*, 4014−4022.
(74) Henkelman, G.; Jónsson, H. Improved Tangent Estimate in the Nudged Elastic Band Method for Finding Minimum Energy Paths and Saddle Points. *J. Chem. Phys.* **2000**, *113*, 9978−9985.
(75) Henkelman, G.; Uberuaga, B. P.; Jónsson, H. A Climbing Image Nudged Elastic Band Method for Finding Saddle Points and Minimum Energy Paths. *J. Chem. Phys.* **2000**, *113*, 9901−9904.
(76) Álvarez-Moreno, M.; de Graaf, C.; López, N.; Maseras, F.; Poblet, J. M.; Bo, C. Managing the Computational Chemistry Big Data Problem: The IoChem-BD Platform. *J. Chem. Inf. Model.* **2015**, *55*, 95−103.
(77) Navarro-Ruiz, J. Data Set for: Prevalence of trans-Alkenes in Hydrogenation Processes on Metal Surfaces: A Density Functional Theory Study. http://dx.doi.org/10.19061/iochem-bd-1-87.
(78) Bahn, S. R.; López, N.; Nørskov, J. K.; Jacobsen, K. W. Adsorption-Induced Restructuring of Gold Nanochains. *Phys. Rev. B* **2002**, *66*, No. 081405.
(79) Calle-Vallejo, F.; Tymoczko, J.; Colic, V.; Vu, Q. H.; Pohl, M. D.; Morgenstern, K.; Loffreda, D.; Sautet, P.; Schuhmann, W.; Bandarenka, A. S. Finding Optimal Surface Sites on Heterogeneous Catalysts by Counting Nearest Neighbors. *Science* **2015**, *350*, 185−189.
(80) Brandt, B.; Fischer, J.-H.; Ludwig, W.; Libuda, J.; Zaera, F.; Schauermann, S.; Freund, H.-J. Isomerization and Hydrogenation of Cis-2-Butene on Pd Model Catalyst. *J. Phys. Chem. C* **2008**, *112*, 11408−11420.
(81) Abild-Pedersen, F.; Greeley, J.; Studt, F.; Rossmeisl, J.; Munter, T. R.; Moses, P. G.; Skúlason, E.; Bligaard, T.; Nørskov, J. K. Scaling Properties of Adsorption Energies for Hydrogen-Containing Molecules on Transition-Metal Surfaces. *Phys. Rev. Lett.* **2007**, *99*, No. 016105.
(82) Studt, F.; Abild-Pedersen, F.; Bligaard, T.; Sørensen, R. Z.; Christensen, C. H.; Nørskov, J. K. Identification of Non-Precious Metal Alloy Catalysts for Selective Hydrogenation of Acetylene. *Science* **2008**, *320*, 1320−1322.
(83) Yang, B.; Burch, R.; Hardacre, C.; Headdock, G.; Hu, P. Origin of the Increase of Activity and Selectivity of Nickel Doped by Au, Ag, and Cu for Acetylene Hydrogenation. *ACS Catal.* **2012**, *2*, 1027−1032.
(84) Yang, B.; Burch, R.; Hardacre, C.; Headdock, G.; Hu, P. Influence of Surface Structures, Subsurface Carbon and Hydrogen, and Surface Alloying on the Activity and Selectivity of Acetylene Hydrogenation on Pd Surfaces: A Density Functional Theory Study. *J. Catal.* **2013**, *305*, 264−276.
(85) Yang, K.; Yang, B. Surface Restructuring of Cu-Based Single-Atom Alloy Catalysts Under Reaction Conditions: The Essential Role of Adsorbates. *Phys. Chem. Chem. Phys.* **2017**, *19*, 18010−18017.

DOI: 10.1021/acs.jpcc.8b06880
J. Phys. Chem. C 2018, 122, 25339−25348